УДК 539.1.074.55

MONTE CARLO SIMULATION OF SILICON DETECTORS FOR THE ALICE EXPERIMENT AT LHC

B.Batyunya, A.Zinchenko

Some results of studies of silicon detector characteristics of the ALICE experiment are presented based on a «realistic» Monte Carlo simulation of the detector performance. The results obtained confirm general conclusions of the Letter of Intent. They also indicate some problems which have to be addressed in order to reach designed parameters.

The investigation has been performed at the Laboratory of High Energies, JINR.

Монте-Карло моделирование кремниевых детекторов для эксперимента АЛИСА на LHC

Б.Батюня, А.Зинченко

Представлены результаты исследований характеристик кремниевых детекторов эксперимента АЛИСА, основанные на «реалистическом» Монте-Карло моделировании их работы. Полученные результаты подтверждают основные выводы проекта эксперимента. Они также указывают на некоторые проблемы, которые должны быть изучены, чтобы достичь запланированных параметров.

Работа выполнена в Лаборатории высоких энергий ОИЯИ.

1. Introduction

In Ref. [1] we described a GEANT-based programme for a «realistic» simulation of silicon detectors of the ALICE experiment and presented some results demonstrating the programme performance. In this paper we show new results obtained during our continuing work on the ALICE silicon detector simulation.

2. Silicon Tracker Geometry

Description of the ALICE detector and simulation programme can be found in Refs. [1] and [2]. The silicon tracker includes five layers of silicon with the innermost layer being a pixel detector, next 3 layers being silicon drift detectors and the outermost one being a double-sided microstrip detector. The pixel detector has a pixel size of 75 μm in r–ϕ and 270 μm in z-direction, the silicon drift detector has the anode pitch of 250 μm (in r–ϕ) and

the drift direction along the beam line with the maximum drift distance of 35 mm, the double-sided microstrip detector has the strip pitch of 100 μm and a stereo angle of 30 mrad. Charge collected on anodes of the silicon drift detector is digitized every 25 ns that corresponds to 150 μm in space for the 6 μm/nc drift velocity.

The following results were obtained using a simple algorithm of cluster finding in silicon detectors, i.e., a cluster was defined as any continuous group of charges exceeding some threshold value. We took the threshold to be equal to 0 for the case without noise added and $4 \times \sigma_{noise}$ otherwise, where σ_{noise} is a standard deviation of the gaussian noise distribution equal to 500 electrons for the pixel and SDDs and $1240e^-$ for the microstrip.

3. Coordinate Resolution of Silicon Drift Detectors

It has been shown in [1] that effect of the electronic noise on coordinate resolution of silicon drift detectors is substantial at least when a coordinate is reconstructed as a simple center of gravity of a charge distributions in a cluster. It means that a good knowledge of noise conditions is essential for correct simulation. As expected in Ref. [3], the noise contribution to sequential time bins in SDDs will be highly correlated. It should result in resolution improvement in z-direction and deterioration in r–ϕ-direction in our case. We checked that by generating the correlated noise according to the two-dimensional gaussian distribution:

$$p(q_i, q_{i+1}) = \frac{1}{2\pi\sigma^2\sqrt{1-\rho^2}} \times \exp\left[-\frac{q_i^2 + q_{i+1}^2 - 2\rho q_i q_{i+1}}{2\sigma^2(1-\rho^2)}\right],$$

$$p(q_1) = \frac{1}{\sqrt{2\pi}\sigma} \times \exp\left[-\frac{q_1^2}{2\sigma^2}\right],$$

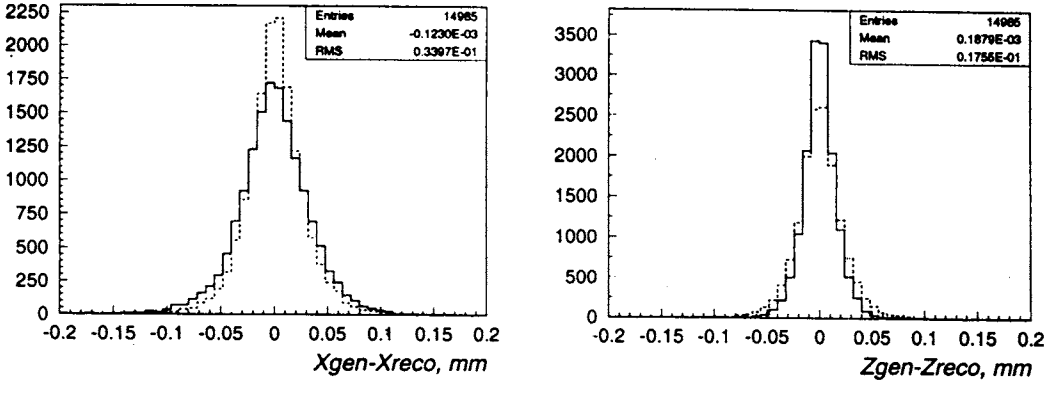

Fig.1. Distributions of «$x_{gen} - x_{reco}$» (left) and «$z_{gen} - z_{reco}$» (right) for silicon drift detectors with a correlated (full line) and uncorrelated (dashed line) noise

where q_1, q_i are noise charges in the first and i-th bins, respectively; σ is a standard deviation of the noise distribution and ρ is a correlation coefficient (we took it equal to 0.95 in our studies). The results obtained are shown in Fig.1, where differences of generated and reconstructed coordinates in azimuthal $(x_{gen} - x_{reco})$ are shown. These distributions were produced for muons with momenta of 6 + 10 GeV/c randomly distributed in angular intervals of $-180° \div 180°$ in ϕ and $85° \div 95°$ in θ. As can be seen, the noise correlation changes the resolution in expected direction.

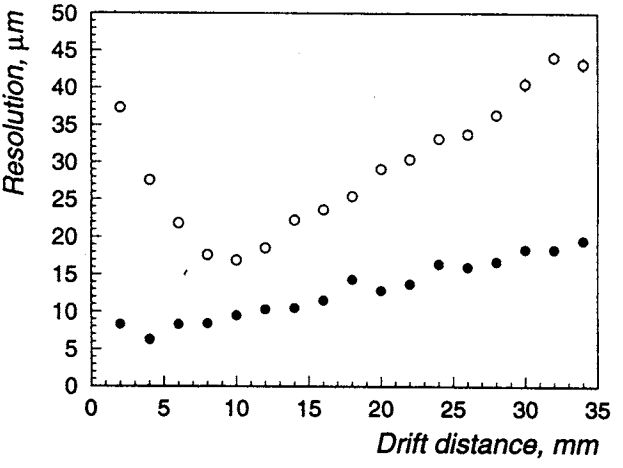

Fig.2. Coordinate resolution of the SDDs with a correlated noise as a function of the drift distance: white circles — r–ϕ-direction, black circles — drift direction

Figure 2 shows coordinate resolution of the SDDs as a function of the drift distance for the case with a correlated noise. The shape of the dependence can be easily understood if one considers the number of anode pads or FADC bins which collect the charge released by a track. The resolution for long drift distances can be possibly improved using more sophisticated methods of coordinate reconstruction [4].

4. *dE/dx*-Measurements in Silicon Detectors

Measurements of energy losses in silicon detectors can contribute to particle identification in the non-relativistic region. Moreover, for low-momentum tracks which do not reach the outer detectors the silicon tracker will be an independent particle spectrometer. Its *dE/dx*-resolution is discussed below. (We considred the pixel detector as a digital device and did not include it in *dE/dx* analysis).

Figure 3 shows distributions of ionization losses in the silicon detectors for muons with momenta of 5 GeV/c and normal angle of incidence without noise added. The results obtained are very close to those in LoI [2] and confirm estimates that *dE/dx*-measurements in the silicon tracker will be able to provide sufficient separation in the regions $p <$ < 140 MeV/c (e/π), $p < 520$ MeV/c (π/K) and $p < 1$ GeV/c (K/p), where «sufficient» means rejection factor of 100 at 95% efficiency. However, the electronics' noise can make the *dE/dx*-resolution worse as shown in Fig.4 for the SDDs and microstrip. One can see that the SDD response is affected significantly due to the fact that some part of the collected charge does not exceed the threshold and the fraction of the lost charge is not constant for all signals.

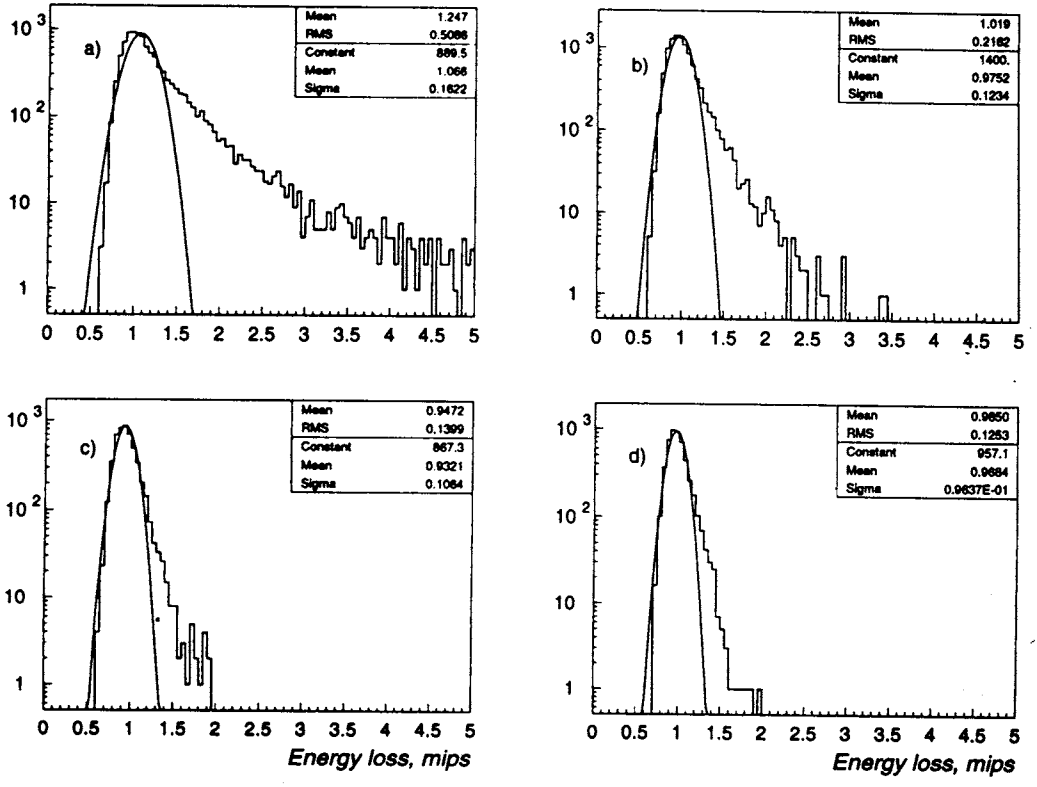

Fig.3. Energy loss distributions in silicon detectors, normalized to 1 at the most probable value. The parameters of a gaussian fit (full lines) around the most probable value are shown in the plots. a) Single detector response to minimum ionizing particle. b-d) Truncated mean using the m lowest of n measurements (b: one of two, c: one of three, d: two of four)

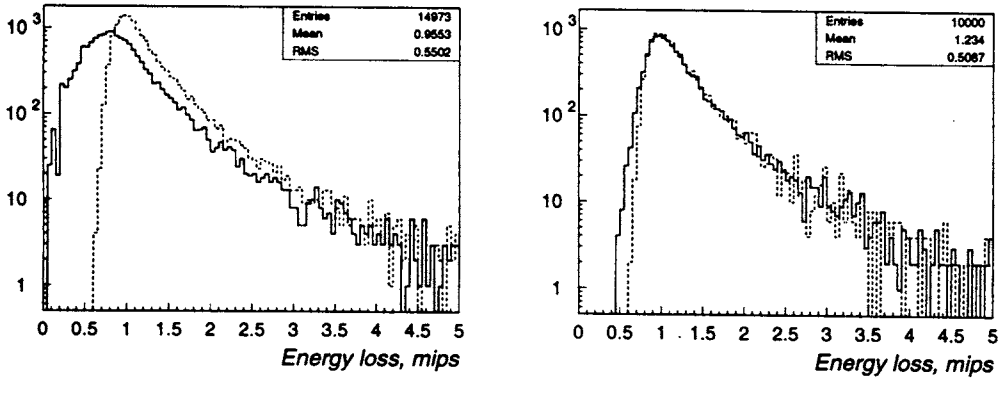

Fig.4. Energy loss distributions in the silicon drift detectors (left) and microstrip (right). Full line — with noise contribution, dashed line — without noise

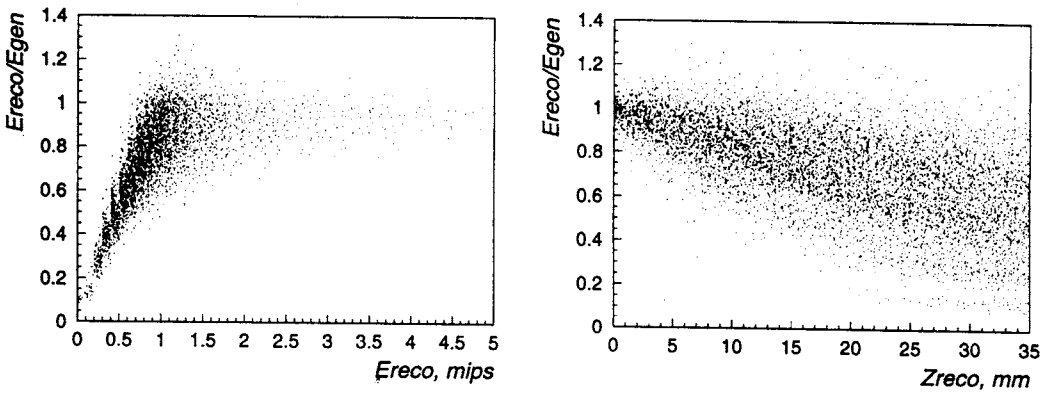

Fig.5. E_{reco}/E_{gen} vs E_{reco} (left) and E_{reco}/E_{gen} vs z_{reco} (right) for 5 GeV/c muons with normal angle of incidence

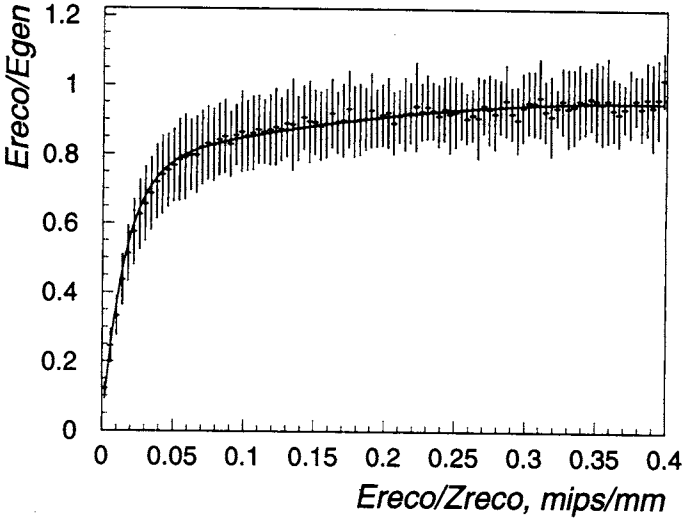

Fig.6. E_{reco}/E_{gen} vs E_{reco}/z_{reco}. The curve shows the result of the fit which was used to correct the detector response

One can try to restore the SDD resolution by introducing corrections. It looks reasonable to assume that the fraction of the lost charge is larger for small signals and long drift distances as can be seen in Fig.5 where a ratio of signals with noise added to those without noise (E_{reco}/E_{gen}) is shown as a function of the signal (E_{reco}) and the drift distance (z_{reco}). We combined these functions into one (Fig.6) and used it to correct the detector response. Figure 7 shows that this procedure works and helps to restore the *dE/ dx*-resolution in the SDDs (at least, partially). After the correction we obtain the rejection factor of 100 at the following efficiencies; 94% (e/π and π/K) and 82% (K/p), whereas without the correction results are significantly worse: 81%, 83% and 65%, respectively.

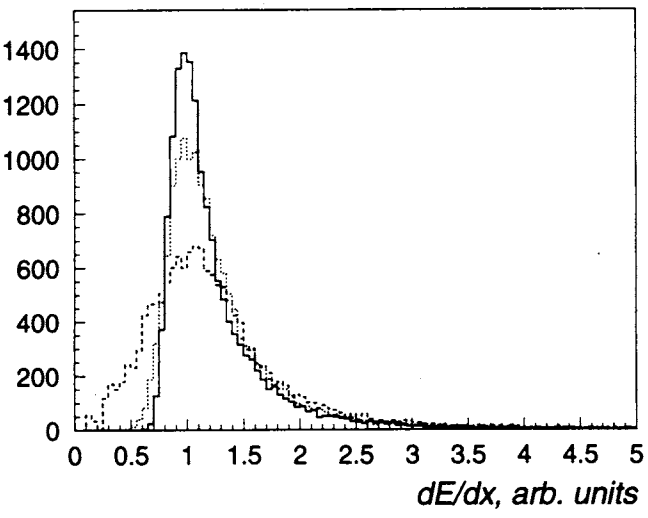

In conclusion it should be noted that this correction procedure might be useful also for gas drift chambers.

Fig.7. Distribution of ionization losses in the SDDs for 5 GeV/c muons with normal angle of incidence, normalized to 1 at the most probable value: solid line — without noise added, dashed line — with noise before correction, dotted line — after correction

5. Multitrack Response

In order to study the silicon tracker capabilities in a multitrack environment we simulated one event of Pb-Pb central collisions with energy of 6.3 TeV/nucleon and charged particle density $dN/dy = 5000$ at $y = 0$ using the HIJING-package [5]. Figure 8 shows lego plots of what we can expect to see from the SDDs in the experiment.

Table 1 shows a distribution of the number of primary charged tracks with $\theta = 50° + 90°$ and momenta greater than 30 MeV/c producing a single cluster. Table 2 is similar to 1 except that all secondary charged tracks produced in the silicon tracker and beam pipe are taken into account. Table 3 is the same as 2 in configuration with additional passive material (support structure and cooling system) included as described in [6].

From a comparison of the tables we can see that the probability for signals from several tracks to overlap is low enough and extra material does not cause very serious problems from the point of view of particle interactions.

Another possible problem is a «ghost» activity in double-sided microstrip detectors with stereo angle. If the distance in r–ϕ-direction between two tracks traversing a detector is smaller than some value (1.5 mm in our case), then fake («ghost») hits appear. We found the average number of «ghost» hits per a real one to be equal to 0.18. This value is not significant and can be further reduced using a correlation of signals from two sides of the microstrip detector [7].

Thus, the current silicon tracker design seems to be adequate for the expected experimental conditions from the point of view of its granularity.

This can be further confirmed by the results on coordinate resolution. Distribtuions of generated and reconstructed coordinates for all charged tracks with momenta > 30 MeV/c are shown in Fig.9. The results shown are consistent with (and close to) the ones for single tracks [1] if the noise correlation in the SDDs (see section 3) and lower average θ-angle

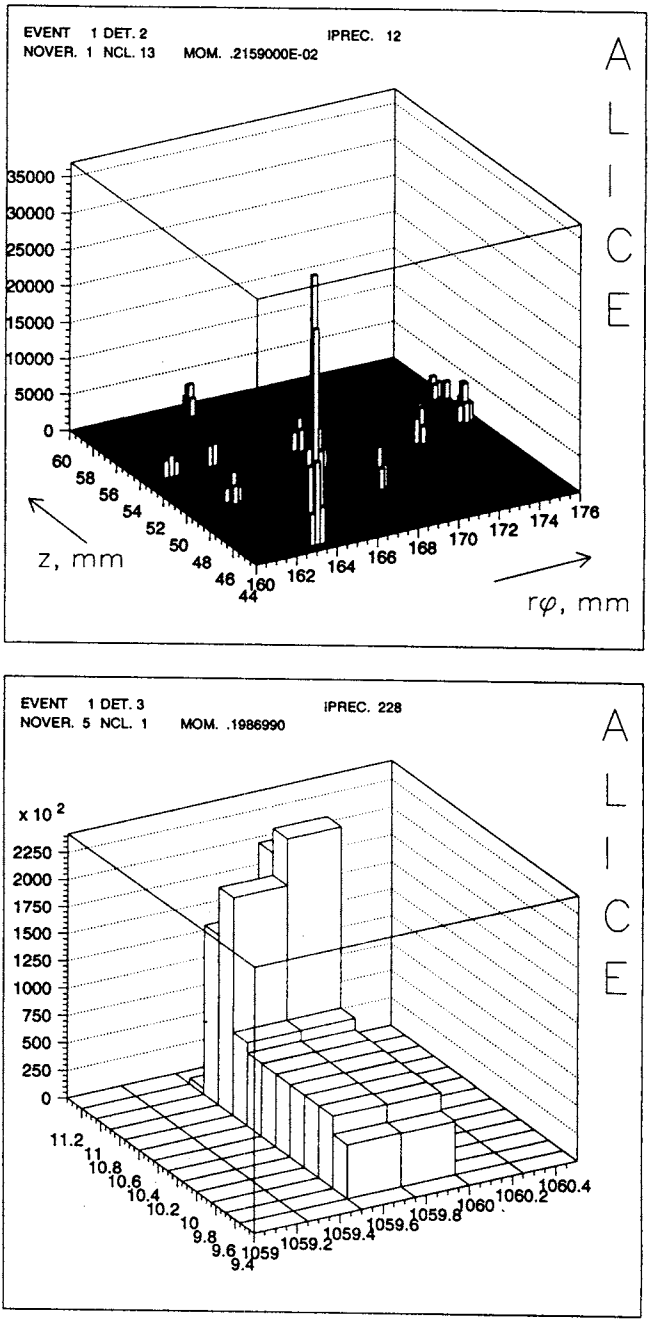

Fig.8. Lego plot of the silicon drift detector response (SDD # 1) to tracks with $\theta \approx 70°$ (top); plot showing a cluster produced by 6 close tracks (bottom)

Table 1. Number of primary charged tracks with θ = 50° ÷ 90° forming a cluster

Detector	Tracks per cluster					Tracks/layer
	1	2	3	> 3	mean	
pixel	3711	41	—	—	1.011	3793
SDD-1	3594	80	2	—	1.023	3760
SDD-2	3654	35	—	—	1.009	3724
SDD-3	3623	8	—	—	1.002	3639
microstrip	3437	86	5	—	1.027	3624

Table 2. The same as in Table 1 for all charged tracks

Detector	Tracks per cluster								Tracks/layer
	1	2	3	4	5	6	> 6	mean	
pixel	3815	54	1	2	1	1	—	1.018	3945
SDD-1	3736	98	3	—	—	—	—	1.027	3941
SDD-2	3854	46	1	1	1	—	1	1.016	3965
SDD-3	3937	18	2	1	—	—	1	1.008	3990
microstrip	3767	119	5	—	—	2	—	1.036	4032

Table 3. The same as in Table 2 in configuration with passive material

Detector	Tracks per cluster								Tracks/layer
	1	2	3	4	5	6	> 6	mean	
pixel	3800	52	2	2	1	—	—	1.017	3923
SDD-1	3748	101	5	—	—	—	—	1.029	3965
SDD-2	3867	58	2	1	2	—	2	1.025	4029
SDD-3	4006	27	—	1	—	—	—	1.007	4064
microstrip	3845	116	6	1	—	—	2	1.037	4118

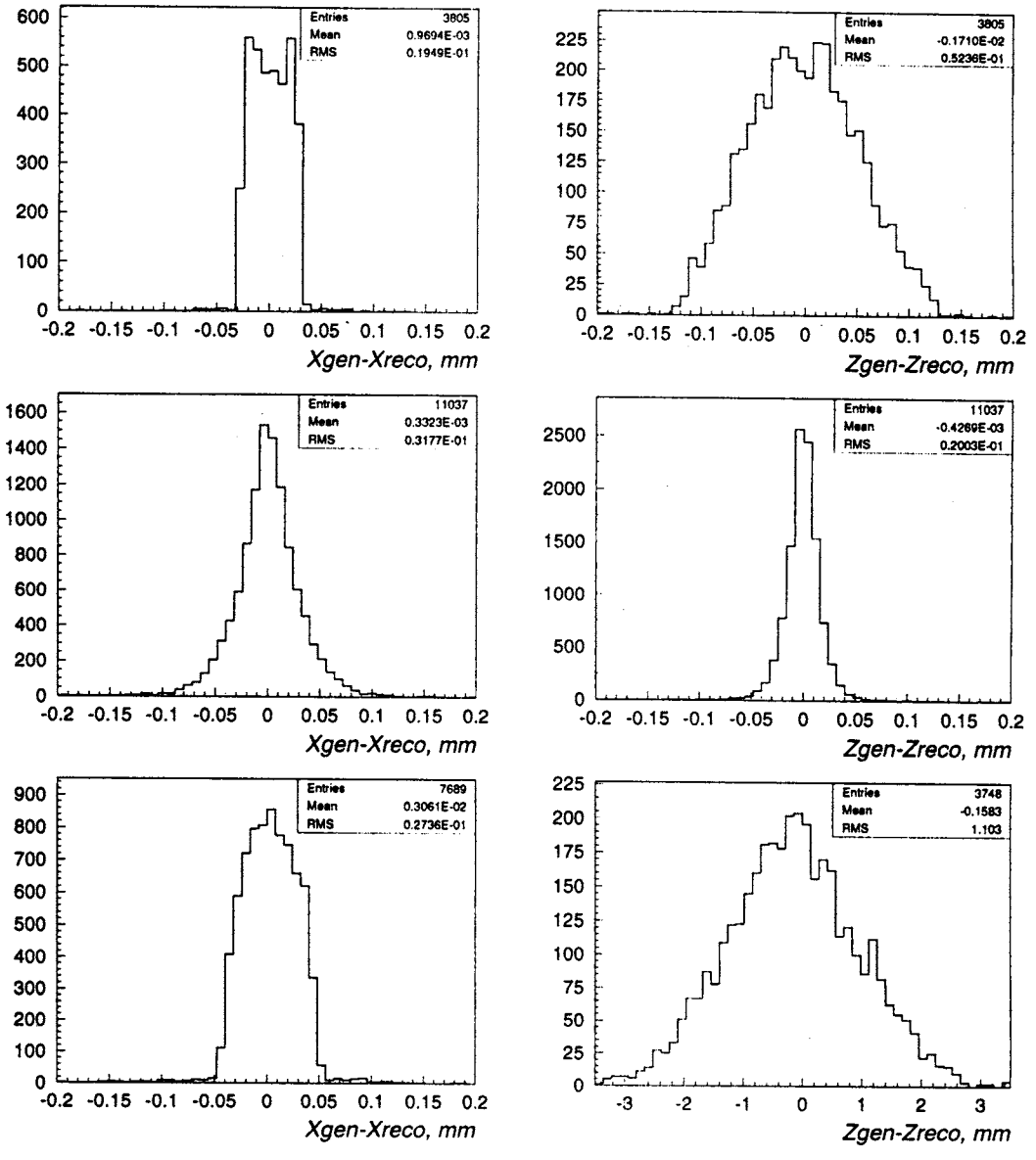

Fig.9. Distributions of the difference of generated and reconstructed coordinates: upper — row-pixel, middle — SDDs, lower — microstrip; left column — r–ϕ-coordinate, right — z-coordinate

(which results in better z-coordinate resolution for the pixel detector) are taken into account. The average cluster size values are shown in Table 4. They are somewhat larger than the ones for single tracks.

Table 4. Average cluster size values for the silicon detectors

Detector	Cluster size	
	r–ϕ-coordinate	z-coordinate
pixel	1.3 (pixels)	1.4 (pixels)
SDD	2.0 (anode pads)	3.0 (FADC bins)
microstrip	1.3 (strips)	

6. Conclusion

The results of the «realistic» simulation of the ALICE silicon tracker performance presented here and in Ref. [1] confirm, in general, conclusions of the LoI [2]. However, they also indicate some problems which have to be addressed in order to reach designed parameters.

References

1. Batyunya B., Zinchenko A. — JINR Communication, E1-94-375, Dubna, 1994.
2. Letter of Intent for a Large Ion Collider Experiment, CERN/LHCC/93-16, LHCC/I4, March 1993.
3. Dabrowski W., Idzik M. — Second-Order Effects in Front-End Electronics and APSP Robustness, Note RD20/TN/15, March 1993.
4. Kozlowski M. et al. — The Resolution of the Linear Silicon Drift Detector Studied by a Computational Model, Internal Note ALICE/94-10, 1994.
5. Wang N.X. et al. — Phys. Rev., 1991, D44, p.3521; Phys. Rev. Lett., 1992, 68, p.1480.
6. Godisov O.N. et al. — Evaporative Cooling for the ALICE Inner Tracker: First Prototype Tests, In: Internal Note ALICE /93-36, Novermber 1993.
7. Monteno M. — Study of the Efficiency of Charge-Matching Methods to Solve Ambiguous Tracks in 2-Sided Silicon Detectors, Internal Note ALICE/94-13

Received on February 24, 1995.